

Saddlepoint adjusted inversion of characteristic functions

Berent Å. S. Lunde *

Tore S. Kleppe †

Hans J. Skaug ‡

November 15, 2018

Abstract

For certain types of statistical models, the characteristic function (Fourier transform) is available in closed form, whereas the probability density function has an intractable form, typically as an infinite sum of probability weighted densities. Important such examples include solutions of stochastic differential equations with jumps, the Tweedie model, and Poisson mixture models. We propose a novel and general numerical method for retrieving the probability density function from the characteristic function. Unlike methods based on direct application of quadrature to the inverse Fourier transform, the proposed method allows accurate evaluation of the log-probability density function arbitrarily far out in the tail. Moreover, unlike saddlepoint approximations, the proposed methodology can be made arbitrarily accurate. Owing to these properties, the proposed method is computationally stable and very accurate under log-likelihood optimisation. The method is illustrated for a normal variance-mean mixture, and in an application of maximum likelihood estimation to a jump diffusion model for financial data. **Keywords** Likelihood estimation Inverse Fourier transform Exact saddlepoint approximation Numerical integration Jump diffusions Mixture models

1 Introduction

This paper is motivated by the problem of making inference about parameters of statistical models, in which the probability density function is not readily available, but the characteristic function (CF) is. Such models appear frequently when there are more than one source of randomness, which is usually the case in the real world;

- (1) The compounded Poisson process and Tweedie model (Tweedie, 1984; Jorgensen, 1987), has a closed form characteristic function, which is usually applied when doing inference.

- (2) The transition distributions of the class of affine jump diffusion models (Duffie et al., 2000) admit characteristic functions given in terms of the solution of certain ordinary differential equations, whereas the transition densities are typically not tractable.
- (3) The solution of non-linear stochastic differential equations (SDE) can be approximated well using Itô-Taylor expansions, for which the characteristic function can be derived (Preston and Wood, 2012). A further extension to the SDE is to add independent stochastic jumps that occur with an intensity at the given time. The new sources of randomness, the counting process and the jump size, can then be easily added to the characteristic function of the approximate solution to the SDE (Zhang and Schmidt, 2016).
- (4) Other important examples include the non-central χ^2 , other Poisson mixtures, Normal mixtures and so on.

Estimation methods based on the CF (or more generally, when the density/mass function is unavailable) can roughly be classified in two groups, based on whether or not the inverse Fourier transform (IFT) is used to compute likelihoods. Popular methods in the latter group include (Generalized) Method of Moments (MM), which seeks to match a finite number of empirical moments with those from the model (see e.g. Hansen, 1982, and subsequent literature). A somewhat similar approach is that of using the empirical characteristic function (ECF), where the idea is to minimize a measure of the difference between the model-implied and empirical characteristic functions (see e.g. Yu, 2004, and references therein).

The MM is computationally very efficient, but as only a finite number of moment conditions are considered, these methods may discard important information from the data. Such information loss does not in theory occur for ECF, but in practice ECF estimators often turn out to have asymptotic inefficiencies (see e.g. Knight et al. (2002, Section 4)).

The former group of methods, e.g. fully likelihood-based methods such as maximum likelihood estimation and Bayesian methods, approximates densities by evaluating IFTs numerically. Direct integration techniques,

*Department of Mathematics and Physics, University of Stavanger, 4036 Stavanger, Norway. Tel.: +47-47258605. berent.a.lunde@uis.no

†Department of Mathematics and Physics, University of Stavanger, 4036 Stavanger, Norway

‡Department of Mathematics, University of Bergen, 5020 Bergen, Norway

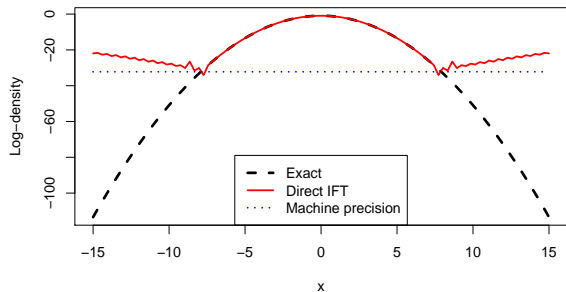


Figure 1: Logarithm of the $N(0, 1)$ density calculated using quadrature-based direct inversion (Direct IFT), along with the exact log-density. Also indicated is $\log(1.0 \times 10^{-14})$.

such as quadrature, will, as illustrated in Figure 1, suffer from numerical inaccuracies that are non-trivial on log-scale in low-density regions. Such problems typically occur when the value of the true density is smaller than around 1.0×10^{-14} , when using double numerics. This is related to the fact that the integrand of the IFT integral takes values $O(1)$. Consequently the weighted sum of integrand evaluations constituting the quadrature approximation will be represented by a floating point number with integer exponent close to 0 (see e.g. Press et al., 1992, Section 1.3, for a discussion of how floating point numbers are represented). The spacing between representable numbers in such a floating point representation (typically on the order 1.0×10^{-16} for exponent close to 0) produces a theoretical lower bound on the magnitude of density values that can be accurately represented. However, from experience, accurate calculation of log-densities via quadrature approximations to the IFT typically fails when the density takes values a few orders of magnitude higher than this bound.

For likelihood-based estimation purposes, it is typically very important that log-densities can be evaluated in a stable manner, even far out in the tails. Therefore, density retrieval for estimation purposes will often involve rescaling properties of the density, such that the IFT is done in a high-density region and then scaled to the point of evaluation. For example, for the mentioned Tweedie model, Dunn and Smyth (2008) elaborate on density retrieval by the IFT using numerical integration. To bypass the problems in the tail, an analytically tractable rescaling property is stated and applied. Moreover, it is commented that satisfactory accuracy is only attained by utilizing this property. Unfortunately, such rescaling properties are not always evident for a general model.

An alternative to direct inversion is the saddlepoint approximation (SPA) (Daniels, 1954; Barndorff-Nielsen and Cox, 1979; Butler, 2007). The SPA often admits

fast computation, is highly automatic and allows for well-scaled numerics when evaluating log-density approximations. In addition, the SPA has been shown to be accurate in the tails of the distribution (see Butler, 2007). However, the SPA suffers some drawbacks in the context of likelihood estimation. Most notably is that it in general does not integrate to 1, and thus may bias SPA-based estimation towards regions of the parameter space where the integral over the SPA is highest. Further, the SPA is unimodal, and may thus produce an inaccurate approximation of e.g. mixtures, which is a typical case in which the characteristic function is readily available but the density is not.

To bypass some of these problems, the SPA can be improved upon by employing a non-Gaussian base (Wood et al., 1993). Ait-Sahalia and Yu (2006) considers this approach for Markov processes, including jump diffusions. However, non-Gaussian based SPA requires the user to select a base-distribution with a density that in some sense is similar to the target density, and therefore may require bespoke implementations in each instance. Kleppe and Skaug (2008) introduce a method for choosing this base-distribution automatically for the purpose of high-dimensional inversion under a latent-variable framework.

In this paper, we propose to precondition the integrand in univariate inversion problems so that quadrature-based inversion is as numerically stable as possible. This is done by inverting a standardised and exponentially tilted (Barndorff-Nielsen and Cox, 1979) version of the target density, so that the inversion is done in a high-density region. The method is completely automatic, and in particular does not rely on known rescaling properties of the target density or the elicitation of a non-Gaussian base distribution.

The rest of the paper is laid out as follows: the proposed method and its implementation are outlined in section 2. In section 3, the proposed methodology is illustrated and contrasted to alternatives using the normal inverse Gaussian distribution and the Merton jump diffusion models as example models. Conclusion and comments follow in section 4.

2 Methodology

This section provides some background and subsequently derives the saddlepoint adjusted IFT method proposed here.

2.1 Background

Suppose that the strictly continuous random variable $X \in \mathbb{R}$ has probability density function $p_X(x)$ and CF $\varphi_X(s) = E_X(\exp(isX))$, where $i = \sqrt{-1}$. As the CF may be considered as a Fourier transform of $p_X(x)$, the

density can be recovered from $\varphi_X(s)$ via an IFT:

$$p_X(x) = \frac{1}{2\pi} \int_{-\infty}^{\infty} \varphi_X(s) e^{-isx} ds. \quad (1)$$

For numerical evaluation, (1) can be simplified by utilizing the Hermitian property of $\varphi_X(s)$:

$$p_X(x) = \frac{1}{\pi} \int_0^{\infty} \text{Re} [\varphi_X(s) e^{-isx}] ds. \quad (2)$$

As explained in the introduction and illustrated in Figure 1, computing the log-density $\log p_X(x)$ by taking the logarithm of the output of a quadrature method applied to either (1) or (2) is problematic when the value of $p_X(x)$ is small. Indeed, from Figure 1 it is seen that evaluation of the $N(0, 1)$ log-density based on direct inversion fails around $p_X = \log(1.0 \times 10^{-14})$ (indicated by the horizontal line).

2.2 Saddlepoint adjusted IFT

In order to avoid such numerical problems when evaluating log-densities, this section introduces a general method of preconditioning the integration problem. The overarching idea is to ensure that every numerical IFT approximates the density of a unit variance random variable at its mean. Modulus strongly pathological cases, this approach should ensure that the value of the numerical Fourier transform is $O(1)$.

Again, suppose X is the random variable of interest. Provided it exists, the cumulant generating function (CGF) $K_X(t)$ is defined as $K_X(t) = \log\{E(\exp(tX))\}$, for values of $t \in \Omega$ where $\Omega = \{t : E(\exp(tX)) < \infty\}$. In particular, the CGF may be recovered from the CF via

$$K_X(t) = \log\{\varphi_X(-it)\}.$$

Suppose one wishes to evaluate p_X at some point, say x_0 . A general and analytically tractable rescaling of the original density p_X is obtained by first introducing an exponentially tilted (see e.g. Butler, 2007, Section 2.4.5) version of X , say $X(\tau)$, where $\tau \in \Omega$ is the tilt parameter. The tilted random variable $X(\tau)$ has density

$$p_{X(\tau)}(x) = \exp(\tau x - K_X(\tau)) p_X(x). \quad (3)$$

Notice in particular that the original random variable X is obtained for $\tau = 0$. Straight forward calculations yield that the CGF associated with $X(\tau)$ is given as

$$K_{X(\tau)}(t) = K_X(t + \tau) - K_X(\tau). \quad (4)$$

Now, in order for the evaluation of $p_{X(\tau)}$ to happen in a high-density region, the tilt parameter $\tau = \hat{\tau}$ is chosen so that $E(X(\hat{\tau})) = x_0$. As $E(X(\tau)) = K'_X(\tau)$, one obtains the saddlepoint equation

$$K'_X(\hat{\tau}) = x_0, \quad (5)$$

for $\hat{\tau}$, where K'_X denotes the derivative of K_X .

A further standardization is then introduced in order to ensure that the target for the numerical IFT also has unit variance (and thus under most circumstances has density values $O(1)$ around the mean). This is achieved by introducing a standardized version of $X(\hat{\tau})$,

$$\bar{X}(\hat{\tau}) = \frac{X(\hat{\tau}) - x_0}{\sqrt{\text{Var}(X(\hat{\tau}))}}, \quad (6)$$

where $\text{Var}(X(\hat{\tau})) = K''_X(\hat{\tau})$, so that

$$p_{\bar{X}(\hat{\tau})}(x_0) = \frac{p_{X(\hat{\tau})}(0)}{\sqrt{K''_X(\hat{\tau})}}. \quad (7)$$

Combining (3) and (7) results in the preconditioning formula used throughout this text, namely

$$p_X(x_0) = \exp(K_X(\hat{\tau}) - \hat{\tau}x_0) \frac{p_{\bar{X}(\hat{\tau})}(0)}{\sqrt{K''_X(\hat{\tau})}}. \quad (8)$$

Since (6) represents an affine transformation of $X(\hat{\tau})$, the CF and CGF of $\bar{X}(\hat{\tau})$ are also easily found to be

$$\begin{aligned} \varphi_{\bar{X}(\hat{\tau})}(s) &= \exp(K_{\bar{X}(\hat{\tau})}(is)), \\ K_{\bar{X}(\hat{\tau})}(t) &= -K_X(\hat{\tau}) - \frac{tx_0}{\sqrt{K''_X(\hat{\tau})}} \\ &\quad + K_X\left(\frac{t}{\sqrt{K''_X(\hat{\tau})}} + \hat{\tau}\right), \end{aligned}$$

and thus density of $\bar{X}(\hat{\tau})$ evaluated at zero can be calculated as

$$p_{\bar{X}(\hat{\tau})}(0) = \frac{1}{\pi} \int_0^{\infty} \text{Re}[\varphi_{\bar{X}(\hat{\tau})}(s)] ds. \quad (9)$$

Before proceeding, notice that the conventional SPA is obtained by substituting $p_{\bar{X}(\hat{\tau})}(0)$ in (8) with the $N(0, 1)$ density evaluated at 0, namely $(2\pi)^{-1/2}$. Thus, it follows from results on tail-exactness of the SPA (Barn-dorff-Nielsen and Kluppelberg, 1999) that also $p_{\bar{X}(\hat{\tau})}(0)$ must converge to $(2\pi)^{-1/2}$ in the tails of p_X . In the high-density regions of p_X on the other hand, $p_{\bar{X}(\hat{\tau})}(0)$ typically takes values somewhat higher than $(2\pi)^{-1/2}$. These properties are illustrated for a normal inverse Gaussian distribution (to be discussed in more detail shortly) in Figure 2. Note that $p_{\bar{X}(\hat{\tau})}(0)$ approaches $(2\pi)^{-1/2}$ in the tails of the distribution, as the SPA has the tail exactness property. Moreover, notice that $p_{\bar{X}(\hat{\tau})}(0)$ remains well scaled $O(1)$ across the support of the density, and is therefore easy to approximate using quadrature.

2.3 Implementation

Provided the CGF/CF of some distribution X , equations (8) and (9) form the basis for implementing the proposed saddlepoint adjusted IFT technique for evaluating (log-)densities at say x_0 . Each evaluation involves the following steps:

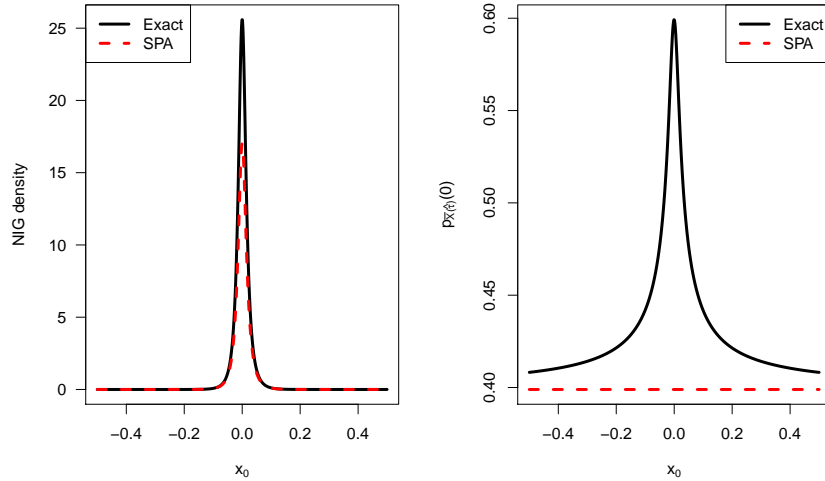


Figure 2: The normal inverse Gaussian (NIG) density along with its SPA (left panel). The right panel shows $p_{\bar{X}(\hat{\tau})}(0)$ (Exact) used in the proposed methodology, together with the asymptote $(2\pi)^{-1/2}$ (SPA). The parameter values $\chi = 0.0003$, $\psi = 1000$, $\mu = -0.0003$, and $\gamma = 2$ in (10) were applied in both plots.

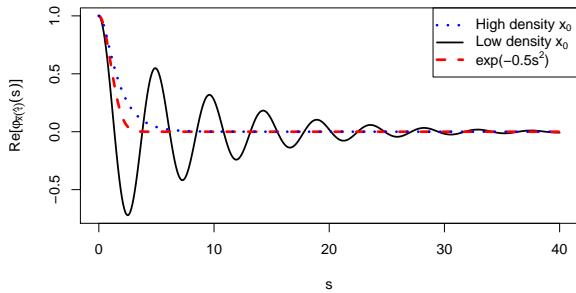


Figure 3: Integrands of the latter representation of (9) for the normal inverse Gaussian distribution. The parameters are the same as in Figure 2. High density x_0 correspond to $x_0 = E(X)$ and low density to $x_0 = E(X) - 8\sqrt{\text{Var}(X)}$. As a reference, also the the CF associated with the $\bar{X}(\hat{\tau})$ obtained whenever X is Gaussian, i.e. $\exp(-s^2/2)$ is indicated. It is seen that the integrands typically take non-negligible values for larger values of s for relative to the Gaussian case.

1. Obtain the saddlepoint $\hat{\tau}$ by solving (5). Notice that $\hat{\tau} = \arg \min_{t \in \Omega} K_X(t) - x_0 t$, where the objective function is convex on Ω . The convexity ensures both a unique such solution to (5), and also that Newton's method of optimization (Press et al., 1992, Chapter 9.4) may be used to obtain a rapidly- and stably converging solution.
2. Approximate the latter integral of (9) by a quadrature approximation, say $\hat{p}_{\bar{X}(\hat{\tau})}(0)$.
3. Compute log-density approximation as

$$\log(p_X(x_0)) \approx K_X(\hat{\tau}) - \hat{\tau}x_0 - \frac{1}{2} \log(K_X''(\hat{\tau})) + \log(\hat{p}_{\bar{X}(\hat{\tau})}(0)).$$

The saddlepoint adjusted IFT comes with some extra cost compared to the saddlepoint approximation and, depending on number of quadrature evaluation, potentially direct IFT. However, for the normal-inverse Gaussian model considered shortly, the location of a single saddlepoint $\hat{\tau}$ per evaluation is a minor part of the required CPU time. This is typically the case even if the saddlepoint equation must be solved numerically, as is often the case for non-trivial models. Thus, of highest importance for good and robust performance is the selection of a quadrature rule for implementing point 2 above.

Figure 3 displays integrands $\text{Re}[\varphi_{\bar{X}(\hat{\tau})}(s)]$ for the normal inverse Gaussian distribution also considered in Figure 2. For values of x_0 in the high-density region of X , the integrand falls to zero rapidly, and the resulting integral may be accurately approximated using Gauss-Hermite quadrature (Press et al., 1992, p. 153). On the

other hand, is seen that the integrand may take non-trivial values far from the origin when x_0 is in the tails of X (even if the resulting integral attains values close to $(2\pi)^{-1/2}$ (Barndorff-Nielsen and Kluppelberg, 1999)).

In the present work, composite Simpson’s quadrature with a fixed integration range is used for the integration problem in point 2 above. This choice is made mainly for robustness and in order to obtain (log-)density approximations that are smooth functions in the parameters. A more adaptive selection of integration range that is also smooth in parameters, and also choosing integration rules that account for the potentially oscillating nature of the integrand holds scope for future research. Notice, however, that such adaptive integration would not alone solve the problems with log-density evaluation for direct IFT as illustrated in Figure 1.

Notice, for comparison, that renormalised (via numerical integration) SPAs require the solution of many saddlepoint equations, while at the same time, introduce non-vanishing approximation errors and loses tail exactness. Thus, due both to a higher computational cost and non-vanishing errors, renormalised SPAs are not considered further here.

Throughout this paper, all methods are implemented in C++ and run in R (R Core Team, 2018) using the RCPP package (Eddelbuettel and François, 2011). Exact gradients of log-likelihood functions were obtained using the automatic differentiation (AD) library Adept (Hogan, 2014). All derivatives of the CGF are hand-coded in the present work, but this process may also be automated using a tool that allows for nested computation of derivatives such as TMB (Kristensen et al., 2016).

3 Illustrations

The focus of this section is to highlight several properties of the saddlepoint adjusted IFT method, and to contrast these to the SPA and direct IFT.

3.1 The Normal inverse Gaussian distribution

Throughout this section, the normal-inverse Gaussian (NIG) (see e.g. McNeil et al., 2005) is used as a test case since this distribution admit exact evaluation of the density. The NIG distribution is defined as a normal-variance mixture,

$$X = \mu + \gamma W + \sqrt{W}Z, \quad Z \sim N(0, 1), \quad (10)$$

where W has an inverse Gaussian distribution with a parametrization corresponding to

$$p_W(w) \propto w^{-3/2} \exp(-(\chi/w + \psi w)/2), \\ E(W) = \sqrt{\chi/\psi} \text{ and } Var(W) = (\sqrt{\chi/\psi})/\psi.$$

The marginal density of X is expressible only in terms of the modified Bessel function of the third kind K_λ :

$$p_X(x) = \frac{\sqrt{\chi(\psi + \gamma^2)} K_{-1} \left(\sqrt{(\chi + (x - \mu)^2)(\psi + \gamma^2)} \right)}{\pi \sqrt{\chi + (x - \mu)^2}} \\ \times e^{\sqrt{\chi}\psi + (x - \mu)\gamma}.$$

On the other hand, the CGF is highly tractable:

$$K_X(t) = s\mu + \sqrt{\chi} \left(\sqrt{\psi} - \sqrt{\psi - s^2 - 2s\gamma} \right).$$

In particular, based on the CGF, one obtains $E(X) = \mu + \gamma\sqrt{\chi/\psi}$ and $Var(X) = \sqrt{\chi}\psi^{-3/2}(\gamma^2 - \psi)$.

In order to implement saddlepoint adjusted IFT, a quadrature scheme must be chosen to approximate $p_{\hat{X}(\hat{\tau})}(0)$ as given in the latter representation of (9). Here, Simpson’s quadrature based on 512 equidistant evaluations in the interval $s \in [0, 100]$ were used throughout. The interval and number of evaluations were chosen to be highly robust for a wide range of parameters and evaluation points x_0 . Notice, that direct IFT on the other hand requires more manual tuning depending on parametrisation.

To illustrate how the saddlepoint adjusted IFT performs under log-likelihood-based estimation, 100 observations from a NIG distribution with parameters $\chi = 0.0003$, $\psi = 1000$, $\mu = -0.0003$, and $\gamma = 2$ were simulated. These parameter values correspond to $E(X) \approx 0.0008$ and $Var(X) \approx 0.023^2$, which are typical of financial returns. The log-likelihood, approximated by saddlepoint adjusted IFT, the SPA, the direct IFT, and using the native R Bessel implementation (regarded as being exact), are plotted in Figure 4 as functions of γ and μ , respectively, while keeping the remaining parameters fixed at the values used for simulation. In both cases it is seen that the direct IFT based on Simpson’s method produces unreliable results for parameter settings far from the “true” parameters. Moreover, the SPA produces a log-likelihood approximation which deviates from the true log-likelihood (Bessel implementation) with a parameter-dependent amount. Hence, the SPA based log-likelihood approximation is likely to result in biases relative to the exact maximum likelihood estimator. Finally, it is seen that the saddlepoint adjusted IFT based approximation is indistinguishable from the true log-likelihood.

To avoid numerical problems resulting from non-positive density approximations, the direct IFT log-likelihood was implemented as $\log(\max(1.0e - 14, \hat{I}))$ where \hat{I} is the quadrature-based approximation of (2). Such non-positive density approximations are obtained as a consequence of a highly oscillating integrand that takes values far larger than the value of the integral itself. Simpson’s quadrature, with 512 function evaluations over the integration range $s \in [0, 150]$, was used. Nevertheless, Figure 4 shows that direct IFT produces erratic behaviour for parameters far from those used in

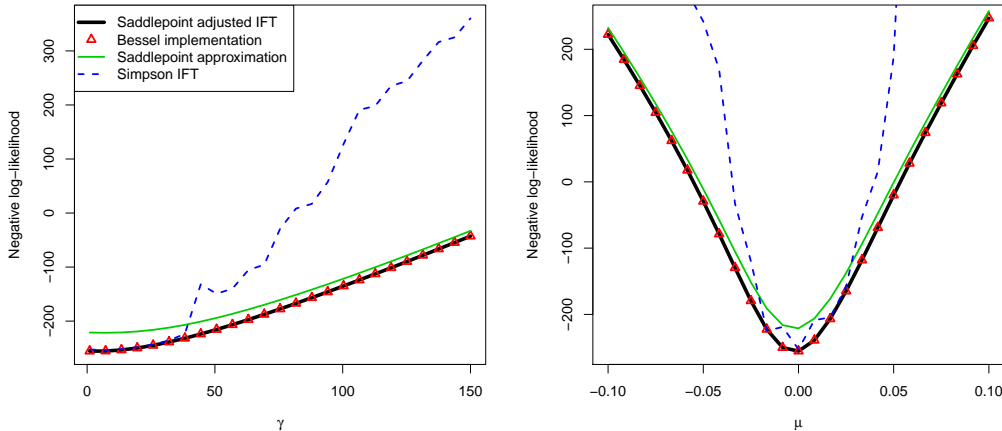


Figure 4: Approximate (negative) log-likelihood profiles based on 100 observations simulated from a NIG distribution with parameter $\chi = 0.0003$, $\psi = 1000$, $\mu = -0.0003$, and $\gamma = 2$. The left panel shows log-likelihoods plotted as a function of γ while keeping the remaining parameters fixed at their “true” values. The right panel shows a similar plot with varying μ .

the simulation. When increasing γ (left panel) the distribution of X changes from being rather symmetric around $\gamma = 2$ to being highly skewed with a heavy right tail and a very thin left tail around $\gamma = 150$. Thus, in this latter case, some of the simulated observations will have very small density values, which is problematic for direct IFT, as demonstrated in Figure 1. Similar reasoning holds for the right panel, where the location parameter μ is varied by around 4 standard deviations in either direction from the “true” μ , and in this case the majority of the simulated data are in the far tails at either extreme of the plot.

As is also seen in Figure 4, the SPA produces approximate log-likelihoods that deviate by a parameter-dependent offset from the exact log-likelihood. This behaviour is related to the fact that the SPA typically does not integrate to 1 (typically < 1), and that the appropriate normalisation factor of the SPA is parameter dependent. However, the SPA is exact in the Gaussian case, and it is therefore often seen (see e.g. Kleppe and Skaug, 2008) that SPA-based parameter estimates are biased towards the “Gaussian part” of the parameter space in models that nest Gaussian distributions. For the NIG distribution, a $N(\mu + \gamma\sigma^2, \sigma^2)$ distribution obtains when $E(W) \rightarrow \sigma^2$ and $Var(W) \rightarrow 0$ (e.g. when $\chi = \sigma^4\psi$ and $\psi \rightarrow \infty$).

To illustrate this effect, we fixed parameters $\mu = \gamma = 0$ and chose $\chi = \psi$ so that $\mathbb{E}[W] = 1$. The remaining free parameter $\theta = 1/\psi = Var(W)$ controls the variance of W , and thus the deviation from normality, with $X \rightarrow N(0, 1)$ as $\theta \rightarrow 0$. We then computed estimators of θ by numerically minimizing the relative Kullback-Leibler divergence to obtain asymptotic maximum like-

lihood estimators,

$$\hat{\theta}(\theta_0) = \arg \min_{\theta} \left\{ - \int \log\{\tilde{p}_X(x; \theta)\} p_X(x; \theta_0) dx \right\}, \quad (11)$$

for different settings of the inverse Gaussian variance θ_0 . Here, \tilde{p} is either the SPA or the saddlepoint adjusted IFT. The integral in the objective function of (11) was resolved using quadrature with 200 evaluations on an interval centered at the mean and spanning 12 standard deviations. The results showed that for the SPA we have $\hat{\theta}(\theta_0) = 0$, i.e. a Gaussian distribution, for all values of θ_0 . For the saddlepoint adjusted IFT, on the other hand, $\hat{\theta}(\theta_0)$ is indistinguishable from θ_0 , i.e. the estimator is asymptotically unbiased.

3.2 Application to real data: Merton jump diffusion

This section considers the application of inversion techniques to likelihood optimisation based on real data. Specifically, the Merton jump diffusion (MJD) (Merton, 1976) for stock prices is considered. Under the MJD model, the dynamics of a stock price S_t are described by the jump diffusion model

$$\frac{dS_t}{S_t^-} = (r - \lambda k)dt + \sigma dW_t + (Y_t - 1)dN_t, \quad (12)$$

where $r > 0$ is the instantaneous expected return on the asset, $\sigma > 0$ the instantaneous volatility (if a jump does not occur), and k the expected relative jump size. N_t denotes a Poisson process with intensity $\lambda > 0$, independent of the Brownian motion W_t . Y_t is the price jump

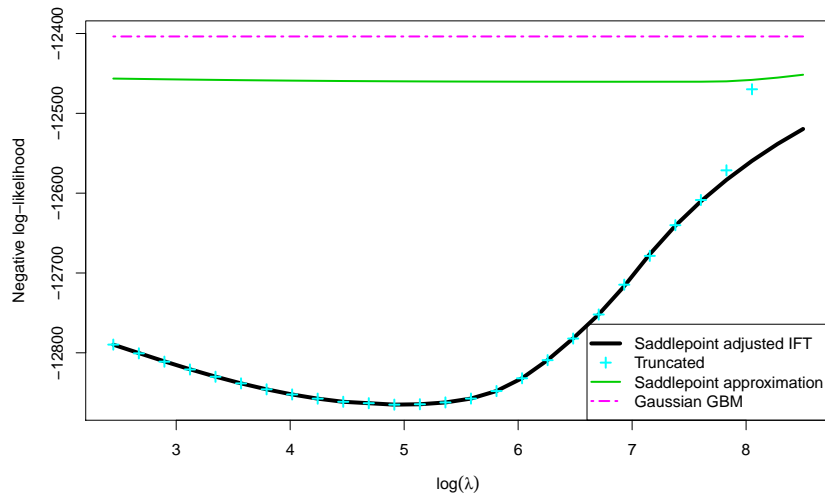


Figure 5: Profile negative log-likelihoods of the Merton Jump Diffusion model versus fixed logarithmic jump-intensities, λ , fitted to DJIA daily stock-market data from 01.01.2000 until 01.01.2018. The evaluations referred to as “Truncated” are obtained by summing conditional probabilities in (15), until either the jump probability is less than 1.0×10^{-14} or reaching 20 jumps. Saddlepoint adjusted IFT uses Simpson’s quadrature with 128 equidistant steps over $s \in [0, 16]$. Direct inversion was deemed infeasible, as it severely suffers from the numerical problems discussed in this article.

	Methods			
	SPI	Truncated	SPA	GBM
r	0.0445 (0.045)	0.0445 (0.045)	0.0432 (0.043)	0.0461 (0.047)
$\log \sigma$	-2.41 (0.077)	-2.41 (0.076)	-2.23 (1.11)	-1.67 (0.011)
$\log \lambda$	4.96 (0.18)	4.96 (0.18)	6.81 (2.36)	
μ	-0.00114 (0.00039)	-0.00114 (0.00039)	-0.000703 (0.00065)	
$\log \nu$	-4.32 (0.074)	-4.32 (0.074)	-5.4 (0.51)	

Table 1: Likelihood estimates and standard deviations in parentheses for the MJD fitted to the DJIA daily stock-market data from 2000 until 2018, applying different methods for likelihood approximation. SPI refers to saddlepoint adjusted IFT. The settings for the methods are the same as those described in Figure 5. The inversion methods were implemented using first order AD data-types with Adept (Hogan, 2014), and Hessian matrices could therefore be retrieved as finite-difference Jacobians to the exact gradients; these could in turn be used to calculate standard deviations (see for instance Kristensen et al. (2016) for details on such computations). The Hessian of the truncation method was retrieved via the `optim` function in R (R Core Team, 2018).

size, meaning that, if a jump occurs at time t , the price jumps from S_{t-} to $Y_t S_{t-}$. The jump sizes Y_t are assumed to be log-normally distributed with $\log Y_t \sim N(\mu, \nu^2)$, and thus $k = e^{\mu+0.5\nu^2} - 1$.

The SDE (12) can be solved to yield the following representation for logarithmic prices:

$$X_t = X_0 + \left(r - \lambda k - \frac{\sigma^2}{2} \right) t + \sigma W_t + \sum_{i=1}^{N_t} \log Y_i, \quad (13)$$

and thus the conditional CGF of $X_t|X_0$ is given as a sum of a normal CGF and a normal compounded Poisson CGF:

$$K_{X_t|X_0}(s) = sX_0 + st \left(r - \lambda k - \frac{\sigma^2}{2} \right) + \frac{s^2 \sigma^2 t}{2} + \lambda t \left(e^{s\mu + \frac{\nu^2 s^2}{2}} - 1 \right). \quad (14)$$

The conditional CGF (14) does not appear to admit a closed form saddlepoint, $\hat{\tau}$, and thus numerical solution of (5) is required.

Notice that the Geometric Brownian Motion (GBM) processes for S_t obtains as special cases either for $\lambda = 0$, or when $\mu = 0$, $\lambda \rightarrow \infty$ and ν decays as $O(\lambda^{-1/2})$ or faster. Furthermore, $X_t|X_0$ is Gaussian under the GBM model.

Note also that for the MJD, $X_t|(X_0, N_t)$ is Gaussian, and thus the exact transition probability density is available as a Poisson mixture with Gaussian components:

$$P(X_t|X_0) = \sum_{i=0}^{\infty} P(N_t = i) P(X_t|X_0, N_t = i). \quad (15)$$

Specifically, $X_t|(X_0, N_t)$ is Gaussian with mean $X_0 + t \left(r - \lambda k - \frac{\sigma^2}{2} \right) + N_t \mu$ and variance $\sigma^2 t + N_t \nu^2$. As a reference for the saddlepoint adjusted IFT, we also consider an approximate log-likelihood function (referred to as ‘‘truncated’’), based on truncating the Poisson mixture infinite sum representation either when the Poisson weights become smaller than $1.0e-14$ or at 20 jumps per transition.

The MJD was applied to stock-market data from the Dow Jones Industrial Average index from 01.01.2000 until 01.01.2018. A yearly time scale, and thus observations separated in time with $t = 1/252$, was used. Maximum likelihood estimation based on saddlepoint adjusted IFT (using Simpson’s quadrature with 128 equidistant evaluations over $s \in [0, 16]$), SPA and the truncated method were considered. Direct IFT was deemed infeasible due to similar problems as discussed above.

Table 1 provides maximum likelihood estimates. First of all, it is seen that the parameter estimates obtained using saddlepoint adjusted IFT and the truncated method are close to indistinguishable. This observation suggests that the proposed methodology performs very well in also this situation, even when using a static integration rule.

The parameter estimates suggest rather frequent jumps at a rate of around 0.6 per day. The jumps have close to zero mean and a standard deviation that is roughly double that of the diffusive part (i.e. $\sigma\sqrt{t}$).

Also included in Table 1 are parameter estimates obtained using a SPA-based log-likelihood approximation. This approximation favours a model with smaller and more frequent jumps, which as discussed above, suggests a model with closer to Gaussian transition distributions. Still, the model obtained using SPA-based log-likelihood is well separated from the exactly Gaussian GBM.

Figure 5 presents negative profile log-likelihoods over $\log(\lambda)$ based on the different considered methods. It is seen that moderate jump intensities, (say below $\log(\lambda) < 7$, $P(N_t = 20 | \log(\lambda) = 7) = 3.1e - 8$), the truncated and saddlepoint adjusted IFT profile log-likelihoods coincide very well, whereas for higher jump intensities, they diverge as the truncation of jump counts starts taking effect. Though not particularly relevant for the data and model at hand here, these observations illustrate the utility of performing the mixing in transform-space, as the computational complexity remains the same for any jump intensity, whereas summing many jumps in the Gaussian mixture representation may become very computationally expensive.

Figure 5 also includes profile likelihoods for SPA-based approximate log-likelihood and the GBM model (invariant of λ). It is seen that the approximate log-likelihood associated with the SPA is substantially closer to the GBM. Notice also that for high jump intensities, the saddlepoint adjusted IFT and SPA approach the GBM as close to Gaussian models are obtained for very high jump intensities are imposed. The truncated method, on the other hand, fails in representing this effect for high jump intensities.

4 Discussion

This paper proposes a new method for numerical inversion of characteristic functions. The proposed method is very reliable for obtaining log-density values, even far out in the tails of the distribution. In particular, the method resolves numerical problems that may occur using direct inverse Fourier transformation. Moreover, the method may be seen as a way of substantially improving the accuracy of the classical saddlepoint approximation when applied in likelihood-based inference.

Further work will involve more automatic rules for choosing integration ranges, under the constraint of producing smooth (in parameters) log-likelihood functions. A further extension would be to consider the low- but multi-dimensional analogue of the proposed methodology. However, more work regarding how to implement the resulting multidimensional integral in point 2 in section 2.3 must be carried out also in this case.

References

- Ait-Sahalia, Y. and J. Yu (2006). Saddlepoint approximations for continuous-time Markov processes. *Journal of Econometrics* 134(2), 507–551.
- Barndorff-Nielsen, O. and D. R. Cox (1979). Edgeworth and saddle-point approximations with statistical applications. *Journal of the Royal Statistical Society. Series B (Methodological)*, 279–312.
- Barndorff-Nielsen, O. E. and C. Kluppelberg (1999). Tail exactness of multivariate saddlepoint approximations. *Scandinavian journal of statistics* 26(2), 253–264.
- Butler, R. W. (2007). *Saddlepoint approximations with applications*. Cambridge University Press.
- Daniels, H. E. (1954). Saddlepoint approximations in statistics. *The Annals of Mathematical Statistics*, 631–650.
- Duffie, D., J. Pan, and K. Singleton (2000). Transform analysis and asset pricing for affine jump-diffusions. *Econometrica* 68(6), 1343–1376.
- Dunn, P. K. and G. K. Smyth (2008). Evaluation of Tweedie exponential dispersion model densities by Fourier inversion. *Statistics and Computing* 18(1), 73–86.
- Eddelbuettel, D. and R. François (2011). Rcpp: Seamless R and C++ integration. *Journal of Statistical Software* 40(8), 1–18.
- Hansen, L. P. (1982). Large sample properties of generalized method of moments estimators. *Econometrica* 50(4), 1029–1054.
- Hogan, R. J. (2014). Fast reverse-mode automatic differentiation using expression templates in C++. *ACM Transactions on Mathematical Software (TOMS)* 40(4), 26.
- Jorgensen, B. (1987). Exponential dispersion models. *Journal of the Royal Statistical Society. Series B (Methodological)*, 127–162.
- Kleppe, T. S. and H. J. Skaug (2008). Building and fitting non-Gaussian latent variable models via the moment-generating function. *Scandinavian Journal of Statistics* 35(4), 664–676.
- Knight, J. L., S. E. Satchell, and J. Yu (2002). Theory & methods: Estimation of the stochastic volatility model by the empirical characteristic function method. *Australian & New Zealand Journal of Statistics* 44(3), 319–335.
- Kristensen, K., A. Nielsen, C. W. Berg, H. Skaug, and B. M. Bell (2016). TMB: Automatic differentiation and Laplace approximation. *Journal of Statistical Software* 70(i05).
- McNeil, A., R. Frey, and P. Embrechts (2005). *Quantitative Risk Management: Concepts, Techniques, and Tools*. Princeton University Press: Princeton, NJ.
- Merton, R. C. (1976). Option pricing when underlying stock returns are discontinuous. *Journal of Financial Economics* 3(1), 125–144.
- Press, W. H., S. A. Teukolsky, W. T. Vetterling, and B. P. Flannery (1992). Numerical recipes in C. *Cambridge: Cambridge University*.
- Preston, S. and A. T. Wood (2012). Approximation of transition densities of stochastic differential equations by saddlepoint methods applied to small-time Itô–Taylor sample-path expansions. *Statistics and Computing* 22(1), 205–217.
- R Core Team (2018). *R: A Language and Environment for Statistical Computing*. Vienna, Austria: R Foundation for Statistical Computing.
- Tweedie, M. (1984). An index which distinguishes between some important exponential families. In *Statistics: Applications and new directions: Proc. Indian statistical institute golden Jubilee International conference*, Volume 579, pp. 604.
- Wood, A. T., J. G. Booth, and R. W. Butler (1993). Saddlepoint approximations to the CDF of some statistics with nonnormal limit distributions. *Journal of the American Statistical Association* 88(422), 680–686.
- Yu, J. (2004). Empirical characteristic function estimation and its applications. *Econometric reviews* 23(2), 93–123.
- Zhang, L. and W. M. Schmidt (2016). An approximation of small-time probability density functions in a general jump diffusion model. *Applied Mathematics and Computation* 273, 741–758.